Contribution from the Lehrstuhl für Anorganische Chemie I, Ruhr-Universität, D-4630 Bochum, FRG,
Institut für Physikalische Chemie, Technische Hochschule Darmstadt, D-6100 Darmstadt, FRG,
and Anorganisch-Chemisches Institut der Universität, D-6900 Heidelberg, FRG

Syntheses and Magnetic Properties of a Heteropolyoxotungsten(VI)iron(III) Cation and $[LFe^{III}(\mu\text{-}MO_4)_3Fe^{III}L]$ Complexes (M = Chromium(VI), Molybdenum(VI)). Crystal Structures of $L_2Fe_2(CrO_4)_3\cdot H_2O$ and $[L_3Fe_3W_4O_{14}(OCH_3)_3](ClO_4)_2\cdot 0.5H_2O$ (L = 1,4,7-Trimethyl-1,4,7-triazacyclononane)

Phalguni Chaudhuri,*† Manuela Winter,† Karl Wieghardt,† Stefan Gehring,‡ Wolfgang Haase,‡
Bernhard Nuber,§ and Johannes Weiss§

Received October 29, 1987

The reaction of $(NH_4)_2CrO_4$ with $LFeCl_3$ (L = $C_9H_{21}N_3$; 1,4,7-trimethyl-1,4,7-triazacyclononane) in water leads to the formation of the tris(μ-chromato)diiron(III) complex $[LFe(\mu\text{-}CrO_4)_3FeL]\cdot H_2O$. The complex crystallizes in the orthorhombic system, space group *Pbca* (D_{2h}^{15}), with lattice constants a = 14.80 (1) Å, b = 15.98 (1) Å, c = 29.22 (3) Å, and Z = 8. Two LFe^{III} units are linked together via three chromate bridges; the geometry around each Fe(III) center, FeN_3O_3, is distorted octahedral. Variable-temperature (4.2–289.5 K) magnetic susceptibility measurements indicate the presence of weakly antiferromagnetically coupled ($2J = -15.0$ (0.4) cm^{-1}) high-spin iron(III) centers. In the molybdenum(VI) analogue $[LFe(\mu\text{-}MoO_4)_3FeL]$, the iron(III) centers interact also in an antiferromagnetic fashion ($2J = -8.8$ (0.4) cm^{-1}), which is very similar to the coupling constant observed for the molybdate-treated pink uteroferrin enzyme. From a reaction mixture consisting of $Fe(ClO_4)_2\cdot 6H_2O$, the cyclic amine 1,4,7-trimethyl-1,4,7-triazacyclononane, and Na_2WO_4 in methanol, brown crystals of $[L_3Fe_3W_4O_{14}(\mu\text{-}OCH_3)_3](ClO_4)_2\cdot 0.5H_2O$ precipitated upon exposure of the solution to air; characterization by X-ray crystallography showed the presence of discrete heteropolyoxotungsten(VI)iron(III) dications and perchlorate anions. It crystallizes in the hexagonal space group $P6_3mc$ (C_{6v}^4, No. 186) with a = 15.764 (4) Å, c = 13.821 (7) Å, and Z = 2. The dication is composed of three LFe^{III} units that are each coordinated via three μ_2-oxo bridges to a $W_4O_{14}(\mu\text{-}OCH_3)_3$ core, yielding three distorted-octahedral *fac*-FeN_3O_3 polyhedra. The iron(III) ions are very weakly antiferromagnetically coupled ($2J = -1.2$ (0.4) cm^{-1}). In the molybdenum(VI) analogue $[L_3Fe_3Mo_4O_{14}(\mu\text{-}OCH_3)_3](ClO_4)_2$, the iron(III) ions are also weakly antiferromagnetically coupled ($2J = -3.8$ (0.4) cm^{-1}).

Introduction

Bridged dinuclear iron complexes attract current attention in view of their biological relevance; they are believed, and in some cases known, to comprise the active centers of various metalloproteins.[1] For this and other reasons we have directed our efforts toward the syntheses of dinuclear iron complexes containing the small tridentate cyclic amine 1,4,7-trimethyl-1,4,7-triazacyclononane (L) as a nonbridging ligand. This cyclic amine coordinates facially in an octahedron and forms thermodynamically and kinetically stable complexes with almost all transition metals in various oxidation states.[2]

The dinuclear iron cluster of uteroferrin in its reduced and enzymatically active pink form is sensitive to a variety of oxyanions,[3] including molybdate, which inhibits the enzyme activity. The pair of irons in the molybdate-treated pink protein are antiferromagnetically exchange coupled with an isotropic coupling constant J of -9 ± 1 cm^{-1}.[3] Apparently, the bridge structure of the dinuclear iron unit remains intact and the binding of molybdate ions occurs at or near the iron centers.

The paucity of molybdate(VI) bridging ligands in iron chemistry is surprising. We have recently reported[4] in a preliminary communication the first tris(μ-molybdato)diiron(III) complex. We have now reinvestigated and extended the magnetic susceptibility measurements of the compound down to 4 K.

Magnetic studies of a considerable number of iron chromates have been well documented in the literature,[5] but without any structural characterization through X-ray diffraction. Rather, a few complexes containing chromium(VI) as the bridging ligand have been unequivocally structurally characterized.[6] One of the subjects of this paper is the synthesis of the tris(μ-chromato)diiron(III) complex containing 1,4,7-trimethyl-1,4,7-triazacyclononane as the terminal ligand, together with its magnetic properties and X-ray structure.

Recent development[7] in the derivative chemistry of early-transition-metal polyoxoanions has opened up new areas in inorganic chemistry. Replacement of peripheral metal–oxygen groups by other metal–ligand complexes and the successful attachment of low-valent organometallic fragments to such polyanions, to name just some of the derivative chemistry, have been reported.[8] These discrete complexes provide well-defined models for examining many of the properties of metal oxide lattices, including magnetic interactions, electron delocalization, and heterogeneous catalysis.[9] The vast majority of these complexes are anions. In a short communication,[4] we recently reported a *cationic* heteropolyoxomolybdenum(VI)iron(III) complex, $[L_3Fe_3Mo_4O_{14}(OCH_3)_3](ClO_4)_2$. We report here the synthesis, magnetic properties, and molecular structure of the tungsten analogue of the above-mentioned heteropolyoxocation, $[L_3Fe_3W_4O_{14}(OCH_3)_3](ClO_4)_2$. We also include the magnetic susceptibility measurements down to 4 K of the molybdenum analogue of the heteropolyoxocation.

Experimental Section

The ligand 1,4,7-trimethyl-1,4,7-triazacyclononane (L) has been prepared by a procedure described previously.[10] All other starting

---

† Universität Bochum.

‡ Technische Hochschule Darmstadt.

§ Universität Heidelberg.

(1) (a) Lippard, S. J. *Angew. Chem.* **1988**, *100*, 353–371, and references therein. (b) Averill, B. A.; Davis, J. C.; Burman, S.; Zirino, T.; Sanders-Loehr, J.; Loehr, T. M.; Sage, J. T.; Debrunner, P. G. *J. Am. Chem. Soc.* **1987**, *109*, 3760–3767 and references therein.

(2) Chaudhuri, P.; Wieghardt, K. *Prog. Inorg. Chem.* **1987**, *35*, 330–436.

(3) Antanaitis, B. C.; Aisen, P. *J. Biol. Chem.* **1985**, *260*, 751–756.

(4) Chaudhuri, P.; Wieghardt, K.; Nuber, B.; Weiss, J. *J. Chem. Soc., Chem. Commun.* **1987**, 1198–1199.

(5) (a) Powers, D. A.; Rossmann, G. R.; Schugar, H. J.; Gray, H. B. *J. Solid State Chem.* **1975**, *13*, 1–13. (b) Mineely, P. J.; Scott, D. L. *Aust. J. Chem.* **1987**, *40*, 387–393 and references therein.

(6) (a) Harel, M.; Knobler, C.; McCullough, T. D. *Inorg. Chem.* **1969**, *8*, 11–13. (b) Gatehouse, B. M.; Guddat, L. W. *Acta Crystallogr., Sect. C: Cryst. Struct. Commun.* **1987**, *C43*, 1445–1447. (c) Bensch, W.; Seferiadis, N.; Oswald, H. R. *Inorg. Chim. Acta* **1987**, *126*, 113–117.

(7) (a) Weakley, T. T. R. *Struct. Bonding (Berlin)* **1974**, *18*, 131–176. (b) Pope, M. T. *Heteropoly and Isopoly Oxometalates*; Inorganic Chemistry Concepts 8; Springer-Verlag: Berlin 1983. (c) Day, V. W.; Klemperer, W. G. *Science (Washington, D.C.)* **1985**, *228*, 533–541.

(8) (a) Komura, A.; Hayashi, M.; Imanaga, H. *Bull. Chem. Soc. Jpn.* **1976**, *49*, 87–91. (b) Knoth, W. H. *J. Am. Chem. Soc.* **1979**, *101*, 759–760. (c) Besecker, C. J.; Day, V. W.; Klemperer, W. G.; Thompson, M. R. *Inorg. Chem.* **1985**, *24*, 44–50. (d) Chorghade, G.; Pope, M. T. *J. Am. Chem. Soc.* **1987**, *109*, 5134–5138 and references therein. (e) Day, V. W.; Klemperer, W. G.; Maltbie, D. J. *J. Am. Chem. Soc.* **1987**, *109*, 2991–3002 and references therein.

(9) Williams, M. M.; Bouchard, D. A.; Hill, C. L. *Inorg. Chem.* **1987**, *26*, 1436–1441 and references therein.

(10) Wieghardt, K.; Chaudhuri, P.; Nuber, B.; Weiss, J. *Inorg. Chem.* **1982**, *21*, 3086–3090.

0020-1669/88/1327-1564$01.50/0

Table I. Summary of Crystal Data and Intensity Measurements

molecular formula	$Fe_2Cr_3C_{18}H_{42}N_6O_{12}\cdot H_2O$	$Fe_2W_4C_{30}H_{72}N_9Cl_2O_{25}$
cryst syst	orthorhombic	hexagonal
a, Å	14.80 (1)	15.764 (4)
b, Å	15.98 (1)	15.764 (4)
c, Å	29.22 (3)	13.821 (7)
V, Å^3	6910 (17)	2974 (3)
Z	8	2
space group	D_{2h}^{15}-*Pbca*	$P6_3mc$ (C_{6v}^4, No. 186)
d, g/cm^3	1.57	2.07
diffractometer	AED II Siemens (graphite monochromator)	
μ(Mo Kα), cm^{-1}	17.7	82.2
2θ range, deg	3–55	3–60
scan type	ω	ω
octants collected	$+h,+k,+l$	$+h,-k,+l$
total no. of reflns	4098	4937
no. of reflns used	3865 [$I \geq 2.5\sigma(I)$]	1417 [$I \geq 2.5\sigma(I)$]
no. of refined params	392	119
transmission factors: min, max	0.75, 1.00	0.25, 1.00
shift/esd: mean, max	0.03, 0.14	0.1, 1.5
residual peaks (max, min), e/Å^3	1.8, −0.56	1.2, −1.2
R^a	6.9	3.5
$R_w{}^b$	6.2	3.4
weighting factor w_i	$1/\sigma^2(F)$	$1/\sigma^2(F)$

[a] $R = \sum||F_o| - |F_c||/\sum|F_o|$. [b] $R_w = [\sum w_i(||F_o| - |F_c||)^2/\sum w_i|F_o|^2]^{1/2}$.

materials were commercially available and were of reagent grade. Microchemical carbon, hydrogen, and nitrogen analyses were performed by Beller Microanalytical Laboratory, Göttingen, West Germany. Infrared spectra were recorded on a Beckman Acculab 10 instrument (KBr disks).

Magnetic susceptibilities of powdered samples were recorded on a Faraday-type magnetometer using a sensitive Cahn RG electrobalance in the temperature range 4.2–289.5 K. The applied magnetic field was ~1.2 T. Details of the apparatus have already been described elsewhere.[11] Experimental susceptibility data were corrected for the underlying diamagnetism. Corrections for diamagnetism were estimated as -204×10^{-6} cm^3/mol of Fe for $L_2Fe_2(CrO_4)_3$, -215×10^{-6} cm^3/mol of Fe for $L_2Fe_2(MoO_4)_3$, -238×10^{-6} cm^3/mol of Fe for the Fe_3Mo_4 cluster, and -246×10^{-6} cm^3/mol of Fe for the Fe_3W_4 cluster. The TIP values[12] for μ-chromato and μ-molybdato compounds were considered to be 207×10^{-6} and 129×10^{-6} cm^3/mol, respectively.

$(C_9H_{21}N_3)FeCl_3$. A solution of $FeCl_3\cdot 6H_2O$ (2.80 g, 10.4 mmol) and the cyclic amine (1.70 g, 10 mmol) in 40 mL of methanol was heated under gentle reflux for 1 h and then allowed to cool to room temperature. The precipitated yellow microcrystals were filtered off, washed with ether, and air-dried; yield 1.68 g (50%). Anal. Calcd (found): C, 32.40 (32.1); H, 6.35 (6.3); N, 12.60 (12.5); Fe, 16.75 (16.6).

$(C_9H_{21}N_3)_2Fe_2(CrO_4)_3\cdot H_2O$. A suspension of $(C_9H_{21}N_3)FeCl_3$ (0.17 g, 0.51 mmol) and $(NH_4)_2CrO_4$ (0.12 g, 0.8 mmol) in distilled water (25 mL) was stirred at 40–45 °C for 2 h. The precipitated deep brown solid was filtered off, washed with a mixture of ethanol–ether (1:2), and air-dried, X-ray-quality red-brown crystals were obtained by recrystallization from an acetonitrile–water mixture; yield 0.25 g (60%). Anal. Calcd (found): C, 26.36 (27.5); H, 5.41 (5.54); N, 10.25 (10.23); Cr, 19.02 (19.4); Fe, 13.62 (13.1).

$[(C_9H_{21}N_3)_3Fe_3W_4O_{14}(OCH_3)_3](ClO_4)_2$. Ferrous perchlorate hexahydrate (0.36 g, 1 mmol) was added to a degassed stirred solution of the cyclic amine (0.51 g, 3 mmol) in 50 mL of methanol under an argon atmosphere. The resulting solution was stirred at room temperature for 2.5 h to give a deep blue color, and a sample of 0.55 g of $Na_2WO_4\cdot 2H_2O$ (1.7 mmol) was added to this solution. The reaction mixture was stirred an additional 1.5 h to obtain a brown solution. After addition of 0.4 g of $NaClO_4\cdot H_2O$ to the brown solution, the mixture was filtered in the presence of air. From the clear solution, kept in a closed vessel, brown crystals of the compound suitable for X-ray crystallography were obtained; yield 0.3 g (47%). Anal. Calcd (found): C, 18.64 (19.4); H, 3.76 (4.0); N, 6.52 (6.6); Fe, 8.67 (9.2); ClO_4, 10.29 (9.5).

$(C_9H_{21}N_3)_2Fe_2(MoO_4)_3$ and **$[(C_9H_{21}N_3)_3Fe_3Mo_4O_{14}(OCH_3)_3](ClO_4)_2$** were prepared according to the described procedures.[4]

Caution! Although we have experienced no difficulties with the perchlorate salts described here, these should be regarded as potentially explosive and handled accordingly.

Table II. Atomic Coordinates for $(C_9H_{21}N_3)_2Fe_2(CrO_4)_3\cdot H_2O$

atom	*x*	*y*	*z*
Fe1	0.6305 (1)	0.1946 (1)	0.1587 (1)
N1	0.7722 (6)	0.2082 (5)	0.1804 (3)
N2	0.6348 (6)	0.1033 (6)	0.2162 (3)
N3	0.6917 (6)	0.0828 (5)	0.1251 (3)
C1	0.7779 (10)	0.1748 (9)	0.2276 (5)
C2	0.7113 (9)	0.1293 (12)	0.2452 (5)
C3	0.6471 (12)	0.0189 (8)	0.1967 (6)
C4	0.6734 (15)	0.0091 (8)	0.1525 (5)
C5	0.7916 (9)	0.0966 (11)	0.1247 (5)
C6	0.8294 (8)	0.1616 (8)	0.1491 (5)
C7	0.7973 (9)	0.2969 (7)	0.1795 (5)
C8	0.5499 (9)	0.1056 (8)	0.2418 (4)
C9	0.6568 (8)	0.0705 (8)	0.0787 (4)
Fe2	0.4107 (1)	0.3682 (1)	0.1053 (1)
N4	0.3954 (6)	0.5055 (6)	0.0972 (3)
N5	0.2747 (6)	0.3884 (5)	0.1362 (3)
N6	0.3260 (7)	0.3777 (6)	0.0420 (3)
C11	0.3270 (9)	0.5282 (9)	0.1342 (6)
C12	0.2634 (12)	0.4763 (8)	0.1482 (5)
C13	0.2092 (9)	0.3595 (14)	0.1022 (5)
C14	0.2320 (9)	0.3651 (11)	0.0556 (5)
C15	0.3448 (13)	0.4589 (9)	0.0238 (5)
C16	0.3660 (12)	0.5248 (9)	0.0504 (5)
C17	0.4834 (8)	0.5470 (9)	0.1033 (5)
C18	0.2625 (9)	0.3402 (8)	0.1770 (4)
C19	0.3563 (10)	0.3160 (9)	0.0088 (5)
Cr1	0.4095 (1)	0.1546 (1)	0.1243 (1)
O1	0.5163 (5)	0.1500 (k)	0.1418 (3)
O2	0.3881 (5)	0.2511 (5)	0.1037 (3)
O3	0.3439 (5)	0.1358 (5)	0.1659 (3)
O4	0.3948 (6)	0.0886 (5)	0.0842 (3)
Cr2	0.6222 (1)	0.3270 (1)	0.0631 (1)
O5	0.6498 (5)	0.2633 (4)	0.1063 (3)
O6	0.5191 (5)	0.3687 (5)	0.0698 (3)
O7	0.6207 (7)	0.2752 (7)	0.0177 (3)
O8	0.6945 (6)	0.3985 (6)	0.0596 (4)
Cr3	0.5376 (1)	0.3700 (1)	0.2065 (1)
O9	0.5946 (5)	0.2790 (4)	0.1992 (3)
O10	0.4626 (5)	0.3817 (5)	0.1640 (3)
O11	0.4833 (6)	0.3682 (6)	0.2518 (3)
O12	0.6073 (6)	0.4453 (5)	0.2066 (3)
aq	0.9678 (12)	0.3242 (11)	0.0683 (6)

Crystal Structure Determinations. The red-brown square-prismatic crystal of $[(C_9H_{21}N_3)_2Fe_2(CrO_4)_3]\cdot H_2O$ used for data collection had dimensions of 0.23 × 0.23 × 0.73 mm and was mounted on a Siemens AED II four-circle diffractometer. Preliminary examinations showed that the crystal belonged to the orthorhombic system, space group D_{2h}^{15}-*Pbca*. The unit cell dimensions were obtained at 22 °C by a least-squares refinement of the angular settings of 27 reflections. The data are summarized in Table I along with details of the treatment of intensity data. The data were corrected for Lorentz and polarization effects. An empirical absorption correction[13] has been carried out (ψ scans). The scattering factors[14] for neutral non-hydrogen atoms were corrected for both the real and the imaginary components of anomalous dispersion. The function minimized during least-squares refinements was $\sum w_i(|F_o| - |F_c|)^2$. The structure was solved by direct methods and refined by full-matrix least squares with the SHELXTL program.[13] Idealized positions of H atoms bound to carbon atoms (C–H = 0.96 Å) were calculated and included in the refinement cycles. All other atoms were refined anisotropically, except the oxygen atom (WA1) of the highly mobile molecule of water of crystallization in the crystal at room temperature; this was refined isotropically. Final positional parameters for all non-hydrogen atoms are given in Table II. Selected bond distances and bond angles are listed in Table III.

A brown pyramidal (0.3 × 0.3 × 0.6 mm) crystal of $[(C_9H_{21}N_3)_3Fe_3W_4O_{14}(OCH_3)_3](ClO_4)_2$ was used for data collection. The unit cell dimensions were obtained at 22 °C by a least-squares refinement of the angular settings (7.8 < 2 θ < 29) of 23 reflections. This Fe_3W_3 cluster is isostructural with the $[(C_9H_{21}N_3)_3Fe_3Mo_4O_{14}(OCH_3)_3](ClO_4)_2$ compound, which has been reported earlier.[4] Both of the dications have

---

(11) Merz, L.; Haase, W. *J. Chem. Soc., Dalton Trans.* **1980**, 875–879.

(12) Tilk, W.; Klemm, W. *Z. Anorg. Allg. Chem.* **1939**, *240*, 355–368.

(13) SHELXTL program package (revision 3, July 1981) by G. M. Sheldrick, Universität Göttingen. Computations were carried out on an ECLIPSE computer.

(14) *International Tables for X-ray Crystallography*; Kynoch: Birmingham, England, 1974; Vol. 4.

Table III. Selected Bond Distances (Å) and Angles (deg) for $(C_9H_{21}N_3)_2Fe_2(CrO_4)_3{\cdot}H_2O$

	Nonbonded Contact		
	Fe1···Fe2	4.552 (5)	
	Coordination Sphere		
Fe1–N1	2.201 (9)	Fe2–N4	2.218 (9)
Fe1–N2	2.225 (9)	Fe2–N5	2.229 (8)
Fe1–N3	2.230 (8)	Fe2–N6	2.241 (10)
Fe1–O1	1.900 (7)	Fe2–O2	1.903 (8)
Fe1–O5	1.907 (7)	Fe2–O6	1.911 (8)
Fe1–O9	1.872 (7)	Fe2–O10	1.890 (8)
N1–Fe1–N2	79.7 (3)	N2–Fe1–N3	78.2 (3)
N1–Fe1–N3	79.6 (3)	N2–Fe1–O1	88.6 (3)
N1–Fe1–O1	163.6 (3)	N2–Fe1–O5	168.4 (3)
N1–Fe1–O5	91.8 (3)	N2–Fe1–O9	90.2 (3)
N1–Fe1–O9	91.0 (3)	N3–Fe1–O1	86.9 (3)
N3–Fe1–O5	92.6 (3)	N3–Fe1–O9	166.1 (3)
O1–Fe1–O5	98.1 (3)	O1–Fe1–O9	100.5 (3)
O5–Fe1–O9	97.8 (3)		
N4–Fe2–N5	79.0 (3)	N5–Fe2–N6	79.6 (3)
N4–Fe2–N6	77.7 (3)	N5–Fe2–O2	89.6 (3)
N4–Fe2–O2	162.3 (3)	N5–Fe2–O6	167.8 (3)
N4–Fe2–O6	91.4 (3)	N5–Fe2–O10	89.0 (3)
N4–Fe2–O10	91.5 (3)	N6–Fe2–O2	87.0 (4)
O2–Fe2–O6	97.9 (4)	N6–Fe2–O6	91.2 (4)
O2–Fe2–O10	101.9 (4)	N6–Fe2–O10	165.6 (4)
O6–Fe2–O10	98.7 (3)		
	Bridging Chromate Groups		
Cr1–O1	1.663 (7)	Cr2–O5	1.672 (7)
Cr1–O2	1.686 (8)	Cr2–O6	1.676 (8)
Cr1–O3	1.582 (8)	Cr2–O7	1.564 (9)
Cr1–O4	1.593 (8)	Cr2–O8	1.569 (10)
Cr3–O9	1.694 (7)	O1–Cr1–O2	109.2 (4)
Cr3–O10	1.677 (8)	O1–Cr1–O3	109.8 (4)
Cr3–O11	1.549 (9)	O1–Cr1–O4	109.1 (4)
Cr3–O12	1.584 (8)	O2–Cr1–O3	109.5 (4)
		O2–Cr1–O4	108.4 (4)
		O3–Cr1–O4	110.8 (4)
O5–Cr2–O6	112.1 (4)	O9–Cr3–O10	109.5 (4)
O5–Cr2–O7	108.7 (4)	O9–Cr3–O11	110.5 (4)
O5–Cr2–O8	109.0 (5)	O9–Cr3–O12	109.1 (4)
O6–Cr2–O7	107.2 (5)	O10–Cr3–O11	106.9 (4)
O6–Cr2–O8	109.8 (5)	O10–Cr3–O12	110.3 (4)
O7–Cr2–O8	109.9 (6)	O11–Cr3–O12	110.6 (5)
Fe1–O9–Cr3	147.1 (5)	Fe2–O10–Cr3	158.1 (5)
Fe1–O1–Cr1	155.4 (5)	Fe2–O2–Cr1	149.1 (5)
Fe1–O5–Cr2	157.0 (5)	Fe2–O6–Cr2	145.7 (5)

Table IV. Atomic Coordinates for $[(LFe)_3W_4O_{14}(OCH_3)_3](ClO_4)_2{\cdot}0.5H_2O$

atom	*x*	*y*	*z*
W1	0.33333	0.66667	0.0
W2	0.40476 (2)	−0.40476 (2)	0.7147 (1)
Fe1	0.2179 (1)	−0.2179 (1)	0.8677 (2)
Cl1	0.0	0.0	0.0904 (12)
O1	−0.2706 (4)	0.2706 (4)	0.4633 (9)
O2	0.33333	0.66667	0.1309 (18)
O3	0.33333	0.66667	0.7720 (14)
O4	−0.2745 (4)	0.2745 (4)	0.1367 (9)
O5	0.8455 (5)	0.3342 (5)	0.2890 (7)
O6	0.4491 (4)	−0.4491 (4)	0.6271 (9)
N1	−0.1480 (6)	0.1480 (6)	0.2894 (14)
N2	0.7387 (8)	0.0855 (8)	0.4560 (12)
CC	0.5188 (18)	0.2594 (9)	0.0363 (25)
C1	0.7637 (17)	0.8030 (22)	−0.1820 (15)
C2	0.2601 (13)	0.2516 (18)	0.4053 (19)
C3	0.6878 (20)	0.7978 (12)	0.0457 (15)
C4	0.3078 (17)	0.1539 (8)	0.1800 (16)
C5	0.9592 (11)	0.3717 (10)	0.4901 (16)
O11	0.0457 (12)	0.0915 (24)	0.1354 (28)
O12	0.0	0.0	−0.0151 (25)
aq	−0.4412 (21)	0.4412 (21)	0.7467 (44)

Table V. Selected Bond Lengths (Å) and Bond Angles (deg) for $[L_3Fe_3W_4O_{14}(OCH_3)_3](ClO_4)_2{\cdot}0.5H_2O$

Fe···Fe	5.461 (6)		
W1–O2	1.810 (25)	Fe1–O1	1.955 (9)
W1–O1	1.786 (4)	Fe1–O5	1.927 (8)
W2–O6	1.713 (9)	Fe1–N1	2.193 (10)
W2–O3	2.105 (7)	Fe1–N2	2.209 (13)
W2–O4	2.101 (8)	O4–CC	1.447 (36)
W2–O5	1.802 (8)		
O2–W1–O1	106.5 (4)	O1b–W1–O1c	112.3 (4)
O1–W1–O1b	112.3 (4)		
O1–Fe1–O5	96.0 (4)	O6–W2–O3	157.1 (6)
O1–Fe1–N1	167.1 (5)	O6–W2–O4	91.3 (4)
O1–Fe1–N2	91.8 (5)	O6–W2–O5	102.1 (4)
O5–Fe1–O5a	94.6 (5)	O3–W2–O4	71.8 (4)
O5–Fe1–N1	92.7 (5)	O3–W2–O5	92.2 (4)
O5–Fe1–N2	168.2 (4)	O4–W2–O4b	82.9 (4)
N1–Fe1–N2	78.2 (6)	O4–W2–O5ab	162.7 (3)
N1–Fe1–N3	78.1 (6)	O4–W2–O5	85.9 (4)
N2–Fe1–N3	77.7 (6)		
W1...W2	4.540 (8)	W2...W2′	3.378 (6)

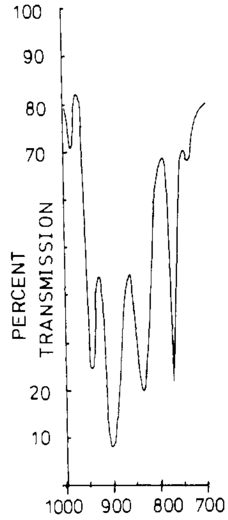

Figure 1. IR spectrum (KBr disk) of $L_2Fe_2(CrO_4)_3$ in the 1000–700-cm^{-1} region.

crystallographically imposed C_{3v} symmetry. The crystallographic data along with details of the treatment of intensity data are in Table I. The data were processed as before, with the exception of hydrogen atoms, which were not included in the refinement cycles. Methoxy carbon atoms (CC) and perchlorate anions (O11, O12) were found to be disordered. They were refined isotropically. Atom coordinates and selected bond distances and angles are listed in Tables IV and V, respectively.

Results and Discussion

Preparation and Characterization of Complexes. In methanolic solutions of the cyclic amine L and $FeCl_3{\cdot}6H_2O$ the yellow monomeric complex $LFeCl_3$ is formed, which reacts in water with ammonium chromate, yielding the red-brown μ-chromato compound $[LFe(CrO_4)_3FeL]$ in good yields.

The reduction in symmetry of the ideally tetrahedral chromate to C_{2v} local symmetry on coordination as a bidentate ligand is reflected in the infrared spectrum. Vibrations due to ν_3 and ν_4 modes are no longer degenerate and should split each to triplets, ν_2 should split to a doublet and ν_1, which is infrared-inactive in T_d symmetry, should be activated in the infrared region. The infrared spectrum of $L_2Fe_2(CrO_4)_3$ consists of a sharp strong band at 780 cm^{-1} and three additional strong bands at 840, 905, and 945 cm^{-1} (Figure 1), which are assigned, on the basis of previous studies[15] of comparable systems, to the ν_1 and ν_3 modes, respectively, of CrO_4^{2-}. The infrared spectrum of $L_2Fe_2(CrO_4)_3$ does not exhibit any absorption attributable to vibrations primarily associated with the bent Fe–O–Cr bridge. The ν_{as}(FeOCr) vibration may be relatively too weak to be observed in the IR spectrum.[23]

---

(15) Coomber, R.; Griffith, W. P. *J. Chem. Soc. A* **1968**, 1128–1131.

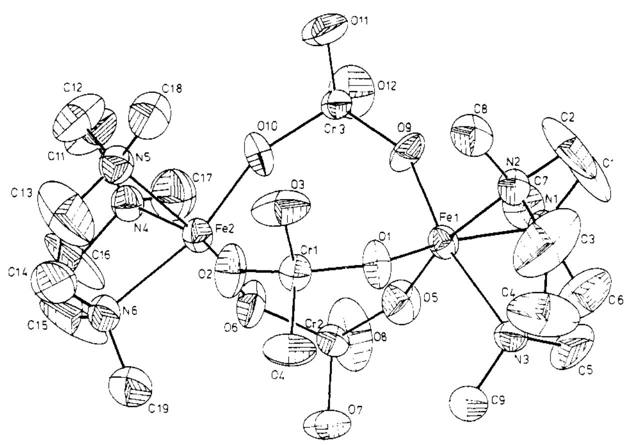

Figure 2. Structure of $[L_2Fe_2(CrO_4)_3]\cdot H_2O$ showing 40% probability thermal ellipsoids and the atom-labeling scheme.

Considering the force constants for Cr–O and Mo–O vibrations to be the same, it is possible to calculate the ν(CrO) frequencies by using the ν(MoO) values observed for $L_2Fe_2(MoO_4)_3$ as described earlier.[4] The calculated values for ν(CrO) are 810, 863, 932, and 974 cm^{-1}, which are significantly greater than those observed experimentally (loc. cit), indicating that Cr–O bonds are more covalent than Mo–O bonds. The last and possibly most informative indication of greater covalency in the μ-chromato compound emerges from the magnetic susceptibility data (vide infra).

The reaction of the blue solution,[16] obtained from $Fe(ClO_4)_2\cdot 6H_2O$ and the cyclic amine in methanol under argon, with tungstate ions affords upon addition of $NaClO_4$ brown crystals of $[L_3Fe_3W_4O_{14}(OCH_3)_3](ClO_4)_2$ in reasonable yields. The complex is sparingly soluble in water with decomposition but reasonably soluble in organic solvents such as acetone, acetonitrile, and alcohols. It is worth noting that besides ligand and ClO_4 absorptions, the IR spectrum of the compound exhibits five sharp strong bands in the region 930–700 cm^{-1} due to ν(WO), $\nu(W_2O)$, and $\nu(W_3O)$.

Description of Structures. $[LFe(\mu\text{-}CrO_4)_3FeL]\cdot H_2O$. The molecular geometry and the atomic labeling scheme are shown in Figure 2. The X-ray structure confirms that a tris(μ-chromato)diiron(III) complex has indeed been formed in such a way that a confacial-bioctahedral geometry containing iron(III) as central atoms is present in the lattice. Three chromate ions bridge the Fe(III) centers in a bidentate fashion. The Fe coordination geometry is distorted octahedral with three nitrogen atoms from the facially coordinated tridentate amine and three oxygen atoms from three bridging chromate groups. Selected bond distances and bond angles are listed in Table III. An Fe···Fe separation of 4.552 (5) Å has been found. The Fe–O (average 1.89 (8) Å) and Fe–N (average 2.224 (9) Å) bond lengths are very similar to those of the model compound[17] for the diiron(III) center in methemerythrin. The largest deviation from idealized 90° interbond angles is 12.9°, which occurs within the five-membered N–Fe–N chelate rings, the N–Fe–N angles ranging between 77.1 (3) and 79.7 (3)°, whereas O–Fe–O angles fall between 97.8 (3) and 101.9 (4)°. The bond lengths are consistent with a d^5 high-spin electron configuration of the Fe(III) centers. The tetrahedral geometry of the chromate anion remains practically unchanged (Table III), even on bridging two Fe(III) centers. Two different types of Cr–O bond distance (averaging 1.678 (8) and 1.574 (9) Å) are observed. Although the C–N bond lengths found in the ligand L are unremarkable (average 1.465 (16) Å), the C–C bond lengths between the methylene groups of the ligand are short (average 1.356 (21) Å) compared to the normal value of 1.54 Å and may be attributed to the effects of libration.

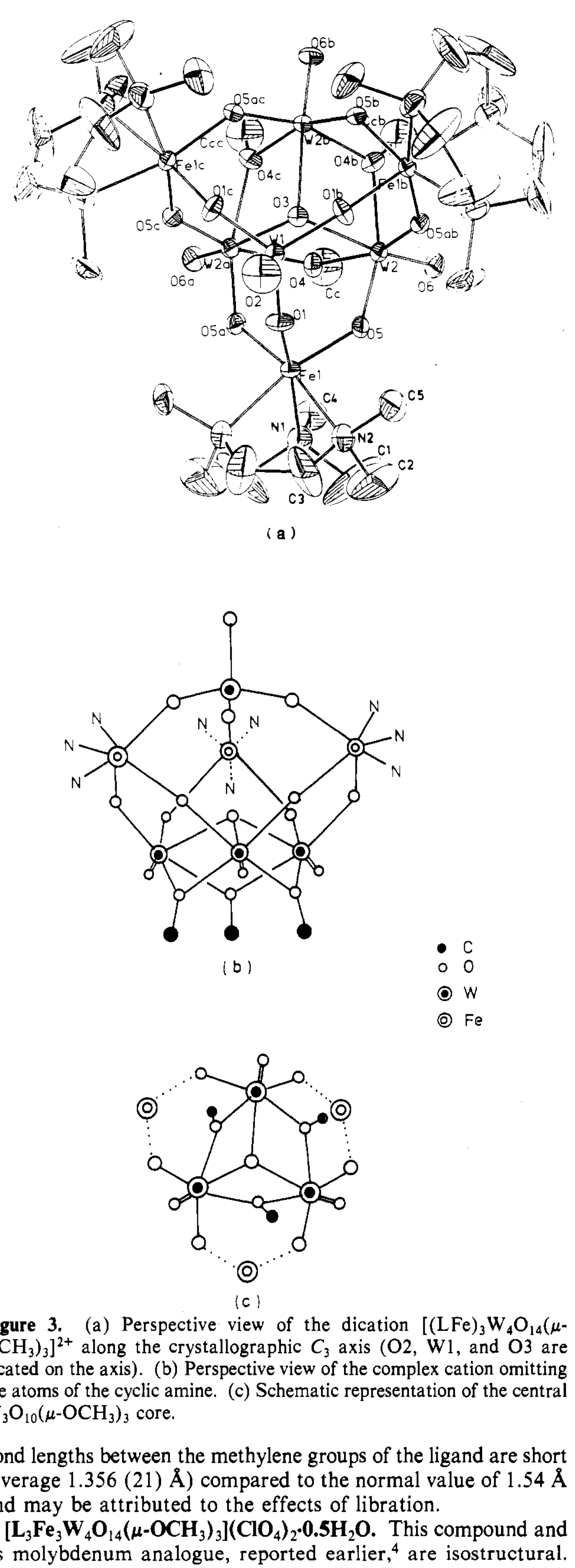

Figure 3. (a) Perspective view of the dication $[(LFe)_3W_4O_{14}(\mu\text{-}OCH_3)_3]^{2+}$ along the crystallographic C_3 axis (O2, W1, and O3 are located on the axis). (b) Perspective view of the complex cation omitting the atoms of the cyclic amine. (c) Schematic representation of the central $W_3O_{10}(\mu\text{-}OCH_3)_3$ core.

$[L_3Fe_3W_4O_{14}(\mu\text{-}OCH_3)_3](ClO_4)_2\cdot 0.5H_2O$. This compound and its molybdenum analogue, reported earlier,[4] are isostructural. Figure 3a shows the complete dication of the Fe_3W_4 cluster, which has crystallographically imposed C_{3v} symmetry. Each of the three LFe^{III} units is coordinated via three μ_2-oxo bridges to a $W_4O_{14}(\mu\text{-}OCH_3)_3$ core (Figure 3b), yielding three distorted-octahedral *fac*-FeN_3O_3 polyhedra. The Fe–N and Fe–O bond distances (Table V) are consistent with a d^5 high-spin electron configuration of the Fe(III) centers. An average Fe···Fe distance of 5.461 (6) Å has been found. The bridging $\mu_3\text{-}WO_4^{2-}$ anion, which also possesses C_{3v} symmetry, is bound to the three LFe^{III} units, and

---

[16] This blue solution affords the mixed-valence dinuclear $Fe^{III}Fe^{II}$ species $[LFe^{III}(OH)_3Fe^{II}L](ClO_4)_2$: Chaudhuri, P.; Pohl, K.; Wieghardt, K., unpublished results.

[17] (a) Chaudhuri, P.; Wieghardt, K.; Nuber, B.; Weiss, J. *Angew. Chem., Int. Ed. Engl.* **1985**, *24*, 778–779. (b) Hartman, J. R.; Rardin, R. L.; Chaudhuri, P.; Pohl, K.; Wieghardt, K.; Nuber, B.; Weiss, J.; Papaefthymiou, G. C.; Frankel, R. B.; Lippard, S. J. *J. Am. Chem. Soc.* **1987**, *109*, 7387–7396.

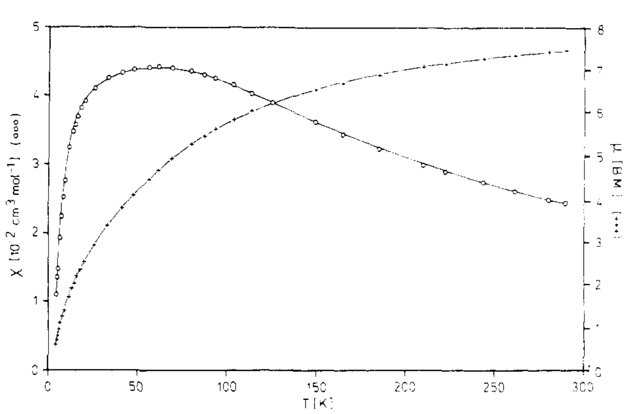

Figure 4. Plots of χ_m and μ_{eff} vs T for solid $L_2Fe_2(CrO_4)_3$. The solid lines are the theoretical least-squares fits to the experimental data.

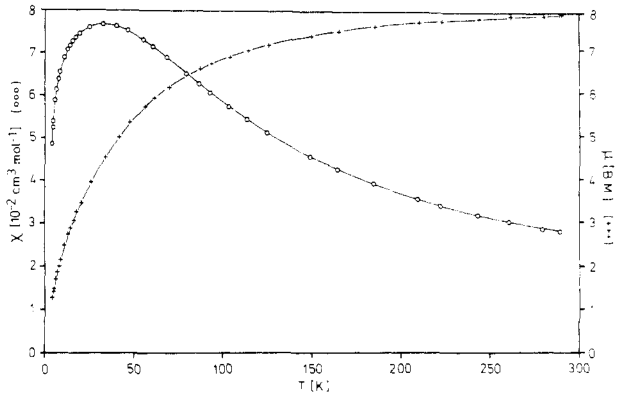

Figure 5. Plots of χ_m and μ_{eff} vs T for solid $L_2Fe_2(MoO_4)_3$. The solid lines represent the best least-squares fits of the experimental data to the theoretical equation.

each of the Fe(III) ions is, in addition, coordinated in a bidentate manner to a central $W_3O_{10}(\mu\text{-}OCH_3)_3$ core (Figure 3c). In the $W_3O_{10}(\mu\text{-}OCH_3)_3$ unit the tungsten(VI) centers are six-coordinate; the W(VI) ions are connected by one μ_3-oxo bridge (O3) and three μ_2-methoxy bridges (O4). Each tungsten has one terminal oxo (O6) ligand. It is to be noted that the average W2···W2′ distance of 3.378 (6) Å is much longer than those found in the $[W_3O_4L_3]^{4+}$ cation[18] (2.477 (3) Å) and $[W_3O_4F_9]^{5-}$ anion[19] (2.514 (2) Å), showing evidently the absence of direct W–W metal bonding due to the nonavailability of d electrons in W(VI) ions. A heteropolytungstate anion containing a bridging methoxy group has been described,[24] but without structural details. To our knowledge this is the first X-ray structurally characterized polytungstate containing bridging methoxy groups. The structural feature of the $W(\mu\text{-}OCH_3)W$ segment is very similar to that of its molybdenum analogue reported earlier.[4] The ClO_4 anions in the crystals were found to be severely disordered.

Magnetic Properties. Variable-temperature (4.2–289.5 K) magnetic susceptibility data were collected for solid samples of $L_2Fe_2(CrO_4)_3$ and $L_2Fe_2(MoO_4)_3$. The magnetic properties of the complexes are displayed in Figures 4 and 5 in the form of molar susceptibility and effective magnetic moment vs temperature. The shape of the susceptibility plot reveals a behavior typical of an antiferromagnetically coupled binuclear compound. The maxima in the susceptibility vs temperature plots of the μ-molybdato (~33 K) and of the μ-chromato compounds (~61 K) are indicative of both longer exchange pathways in the former compound and greater covalency in the chromate anion. The μ_{eff}/Fe values over the temperature range vary from 0.43 μ_B at 4.2 K to 5.30 μ_B at 289.5 K for the chromato-bridged compound and from 0.91 μ_B at 4.2 K to 5.67 μ_B at 289.5 K for the molybdato-bridged compound. The susceptibility data were fitted by means of least squares to the formula (see below) for the paramagnetic susceptibility, which results from the spin Hamiltonian ($\hat{H} = -2J\hat{S}_1\cdot\hat{S}_2$) for isotropic magnetic exchange with $S_1 = S_2 = {}^5/_2$. A correction for a small amount of Curie-law paramagnetic impurity was also taken into account. The expression used is

$$\chi_{\text{calcd}}{}^{\text{dimer}} = (1 - P)\left[\frac{C}{T - \Theta}f(J,T)\right] + P\frac{C}{T} + \text{TIP}$$

where P is the percent of the paramagnetic impurity, $C = Ng^2\mu_B{}^2/k$, and $f(J,T)$ is as given in the literature.[20] The least-squares fits of very good quality are also shown in Figures 4 and 5. The results are summarized in Table VI. Thus, chromate-containing species have enhanced exchange interactions relative to those of species containing molybdate. This is in accord with expectation on the basis of greater covalency in the chromate ion, which presumably stems from the greater electron density on oxygen in the chromate ion as a consequence of the lower electronegativity of chromium when compared with that of molybdenum. Accordingly, the molybdato bridging unit exhibits an unfavorable character to transmit the electronic effects owing to the very low electron density delocalization on the bridging unit of each magnetic orbital. These data also show a higher degree of covalency in the iron–oxygen bonds of the μ-chromato compound than that in the μ-molybdato compound.

Table VI. Magnetic Parameters for Dinuclear and Trinuclear Iron Complexes

compd	J/cm^{-1}	g	Θ/K	P
$[LFe^{III}(\mu\text{-}Cr^{VI}O_4)_3Fe^{III}L]$	−7.5 (2)	2.00 (1)	−0.5	0.4
$[LFe^{III}(\mu\text{-}Mo^{VI}O_4)_3Fe^{III}L]$	−4.4 (2)	2.02 (1)	−1.0	1.1
$[L_3Fe^{III}{}_3Mo^{VI}{}_4O_{14}(OCH_3)_3](ClO_4)_2$	−1.9 (2)	1.98 (2)	0	1.1
$[L_3Fe^{III}{}_3W^{VI}{}_4O_{14}(OCH_3)_3](ClO_4)_2$	−0.6 (2)	2.02 (2)	1.6	0

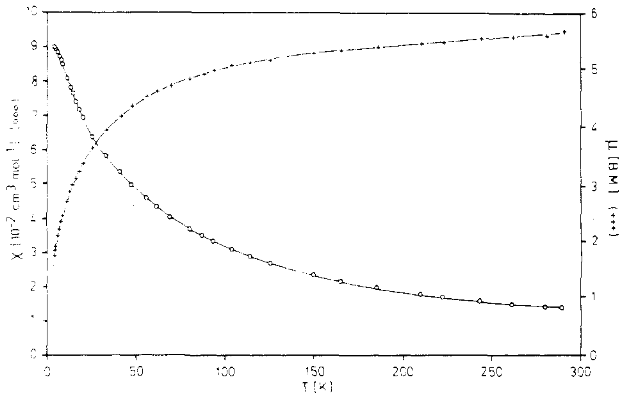

Figure 6. Plots of χ_m and μ_{eff}/Fe vs T for solid $[L_3Fe_3Mo_4O_{14}(OCH_3)_3](ClO_4)_2$. The solid lines are theoretically calculated.

The observed ⟨g⟩ values are very close to the free-electron spin value of 2.00, showing that the iron atoms are in a $^6A_1$ ground state with practically no contribution from orbital angular momentum.

The Fe–Fe separation of 4.552 (5) Å in $[LFe(\mu\text{-}CrO_4)_3FeL]$ is so large that the origin of the exchange integral cannot lie in direct Fe–Fe interaction. Thus, the observed spin coupling is likely to arise through a superexchange mechanism operating via the Fe–O–Cr–O–Fe linkages. A similar argument should also account for the magnetic exchange pathways in the case of the μ-molybdato-bridged diiron(III) complex.

The changes in the optical and EPR spectra of the molybdate-treated pink uteroferrin enzyme have been ascribed to a conformational change of the protein.[3] We wish to point out in this connection that the exchange coupling constant of −9 ± 1 cm^{-1} for the molybdate-induced pink uteroferrin may also be the result of the presence of molybdato-bridged diiron(III) centers. The $2J$ value for our tris(μ-molybdato)diiron(III) complex is very

---

(18) Chaudhuri, P.; Wieghardt, K.; Gebert, W.; Jibril, I.; Huttner, G. *Z. Anorg. Allg. Chem.* **1985**, *521*, 23–36.

(19) Mattes, R.; Mennemann, K. *Z. Anorg. Allg. Chem.* **1977**, *437*, 175–182.

(20) O'Connor, C. J *Prog. Inorg. Chem.* **1982**, *29*, 203–283.

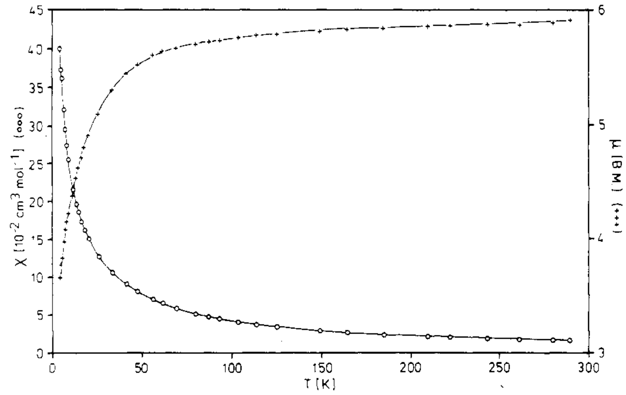

Figure 7. Plots of χ_m and μ_{eff}/Fe vs T for solid $[L_3Fe_3W_4O_{14}(OCH_3)_3](ClO_4)_2$. The solid lines are the theoretical least-squares fits to the experimental susceptibility data.

similar to the above-mentioned coupling constant.

The temperature dependence of the molar magnetic susceptibilities for Fe_3Mo_4 and Fe_3W_4 clusters is shown in Figures 6 and 7. The μ_{eff}/Fe values vary from 1.74 μ_B at 4.2 K to 5.68 μ_B at 289.5 K for the Fe_3Mo_4 compound and from 3.66 μ_B at 4.2 K to 5.91 μ_B at 289.5 K for the Fe_3W_4 compound. Three iron atoms in both compounds are arranged at the corners of an equilateral triangle (see the X-ray structures), each assumed to be in a $^6A_1$ ground state with no contribution from orbital angular momentum. Accordingly, the susceptibility data were fitted by means of least squares to the theoretical expression[21] for χ_M for a symmetrical triangulated trinuclear complex with $J_{12} = J_{23} = J_{31} = J$, which results from the spin Hamiltonian

$$\hat{H} = -2J(\hat{S}_1 \cdot \hat{S}_2 + \hat{S}_2 \cdot \hat{S}_3 + \hat{S}_3 \cdot \hat{S}_1)$$

for an isotropic magnetic exchange with $S_1 = S_2 = S_3 = {}^5/_2$. A correction for a small amount of Curie-law paramagnetic impurity was taken into account by using the expression

$$\chi_{calcd}^{Fe_3\ cluster} = (1 - P)\left[\frac{C}{T - \Theta}f(J,T)\right] + P\frac{C}{T}$$

where the symbols have their usual meanings (loc. cit). The observed exchange coupling constants together with other magnetic parameters are listed in Table VI. The data show that the iron atoms are very weakly coupled in the Fe_3Mo_4 cluster and practically noncoupled in the Fe_3W_4 cluster, as expected on the basis of the degree of covalency in the Fe–O–M (M = Mo or W) bonds. The Fe···Fe separations of 5.445 and 5.461 Å, in the Fe_3Mo_4 and Fe_3W_4 clusters, respectively, are so large that the origin of the exchange integral cannot lie in direct Fe–Fe interaction.

It has been pointed out[22] that the relationship $T_N = -2zJS(S + 1)/3k$, where z is the number of other magnetic ions with which exchange takes place, holds, at least approximately. We calculated T_N values for the Fe_3Mo_4 and Fe_3W_4 clusters to be ca. 5.5 and ca. 1.7 K, respectively. These small values of Néel temperatures are in agreement with the observation that even at 4.2 K the lowest spin level $S' = {}^1/_2$ is not appreciably occupied but its higher lying levels are populated according to their statistical weights for these Fe_3 clusters.

Conclusion

(i) The spin coupling in the studied compounds occurs through the bridging oxyanions in the order

$$|J_{CrO_4}| > |J_{MoO_4}| > |J_{WO_4}|$$

which could be rationalized on the basis of degree of covalency in the Fe^{III}–O–M^{VI}–O–Fe^{III} (M = Cr, Mo, or W) linkages and the length of the exchange pathways.

(ii) The coupling constant (2*J*) of the molybdato-bridged diiron(III) complex is very similar to that of the molybdate-treated pink uteroferrin enzyme.[3] Similar studies on other molybdato-bridged diiron centers, which are in progress in our group, may have a direct bearing on our understanding of the molybdate-induced deactivation of the pink uteroferrin.

(iii) Heteropoly oxometal *cations*, containing $Fe^{III}{}_3M_4O_{14}$ cores (M = Mo^{VI} or W^{VI}) and bridging methoxy groups, have been synthesized. The high-spin iron(III) centers are very weakly antiferromagnetically coupled in the Fe_3Mo_4 cluster and practically uncoupled in the Fe_3W_4 cluster.

Acknowledgment. We thank the Fonds der Chemischen Industrie for financial support of this work.

Registry No. (L)$FeCl_3$, 110827-37-7; $[(L)_2Fe_2(CrO_4)_3]\cdot H_2O$, 113509-05-0; $[(L)_3Fe_3W_4O_{14}(OCH_3)_3](ClO_4)_2\cdot 0.5H_2O$, 113533-03-2; $(L)_2Fe_2(MoO_4)_3$, 111215-31-7; $[(L)_3Fe_3Mo_4O_{14}(OCH_3)_3](ClO_4)_2$, 111241-49-7.

Supplementary Material Available: Tables of bond angles, intraligand bond distances, anisotropic thermal parameters, and calculated positional parameters of H atoms for $L_2Fe_2(CrO_4)_3\cdot H_2O$ and a table of anisotropic thermal parameters for $[(LFe)W_4O_{14}(OCH_3)_3](ClO_4)_2$ (6 pages); listings of observed and calculated structure factors for the two compounds (32 pages). Ordering information is given on any current masthead page.

---

(21) Adams, R. W.; Barraclough, C. G.; Martin, R. L.; Winter, G. *Inorg. Chem.* **1966**, *5*, 346–350.

(22) Earnshaw, A.; Figgis, B. N.; Lewis, J. *J. Chem. Soc. A* **1966**, 1656–1663.

(23) Spool, A.; Williams, I. D.; Lippard, S. J. *Inorg. Chem.* **1985**, *24*, 2156–2162.

(24) Knoth, W. H.; Harlow, R. L. *J. Am. Chem. Soc.* **1981**, *103*, 4265–4266.